Archives of Materials Science and Engineering

Volume 34
Issue 1
November 2008
Pages 35-38

International Scientific Journal
published monthly by the
World Academy of Materials
and Manufacturing Engineering

The microstructure and properties of a new $Fe_{41}Ni_{39}P_{10}Si_5B_5$ glass forming alloy

K. Ziewiec [a,*], K. Bryła [a], A. Ziewiec [b], K. Prusik [c]

[a] Pedagogical University, ul. Podchorążych 2, 30-084 Kraków, Poland
[b] Faculty of Metallurgy and Materials Science, University of Mining and Metallurgy, Al. Mickiewicza 30, 30-059 Kraków, Poland
[c] University of Silesia, ul. Bankowa 12, 40-007 Katowice, Poland
* Corresponding author: E-mail address: kziewiec@ap.krakow.pl

Received 14.08.2008; published in revised form 01.11.2008

ABSTRACT

Purpose: The aim of the work was to investigate the microstructure, thermal stability and some mechanical properties of a new $Fe_{41}Ni_{39}P_{10}Si_5B_5$ glass forming alloy.

Design/methodology/approach: A five component $Fe_{41}Ni_{39}P_{10}Si_5B_5$ alloy was produced using arc melting in argon protective atmosphere from of pure elements 99.95 wt. % Fe, 99.95 wt. % Ni, 99,999 wt. % Si and Fe-P, Fe-B, Ni-P, Ni-B master alloys. The alloy was melt spun. The microstructure of the arc melted droplet is investigated in scanning electron microscope with EDS. The melt spun ribbon was investigated by X-ray diffraction, micro-hardness measurement, dynamic mechanical analysis (DMA), differential scanning calorimetry (DSC) and the microstructure of the melt spun ribbon at the beginning of crystallization process was observed using high resolution transmission electron microscope (HRTEM).

Findings: The arc-melt alloy consisted of four phase constituents that provided amorphization during the melt spinning process. The alloy has relatively high hardness of 720HV and the elastic modulus on the level of 102 GPa. The elastic modulus is stable up to ca. 500 K and after it shows glass transition at 603 K. Crystallization causes temporary increase of the elastic modulus and finally causes brittleness of the sample. The crystallization was found to have the two stages and it begins with formation of bcc iron-base nano-metric crystals.

Research limitations/implications: It has been shown that the multi-component Fe-Ni-P-Si-B system provides the multiphase composition and enables relatively easy amorphization of the $Fe_{41}Ni_{39}P_{10}Si_5B_5$ alloy through the melt-spinning method. It is also possible to control the microstructure and the mechanical properties through the appropriate heat treatment. The existence of glass transformation in the alloy provides possibility of consolidation non-bulk material into a bulk sape.

Practical implications: The work reports about the glass forming alloy of relatively good mechanical properties produced from a low-cost commercial purity precursors. The future investigations on the alloy can provide the basis to the processing and manufacturing soft-magnetic bulk parts of a very low coercivity.

Originality/value: The study provides an original information about the primary structure of the arc-melt $Fe_{41}Ni_{39}P_{10}Si_5B_5$ alloy as well as about the microstructure, mechanical properties and thermal stability of melt-spun ribbon.

Keywords: Amorphous materials; Mechanical properties; Arc melting; Melt spinning

PROPERTIES

1. Introduction

Metallic amorphous alloys are interesting category of materials with very promising mechanical, electric and magnetic characteristics [1-5]. On the other hand, the applications of metallic glasses and amorphous/crystalline composites are still restricted due to high purity and a high price of the precursors. There are also limitations caused by requirements to use an expensive equipment applied to obtain the high purity of the production process. However, it is relatively easy to obtain the amorphous or nanocrystalline ribbon and powder in many systems. The knowledge about the thermal stability is essential both, as regards potential use and possibility of consolidation at elevated temperatures [6, 7]. Especially important is the temperature range of supercooled liquid region $\Delta T=T_x-T_g$, because it provides information on possibility of consolidation as well as stability of mechanical properties e.g.: elastic modulus. It is known that the quaternary Fe-Ni-P-B and Fe-Co-B-Si-Nb systems provide an amorphous very soft magnetic material [8, 9]. Recently, there has been prepared an amorphous alloy based on the Fe-Ni-P-Si-B system e.g.: $Fe_{41}Ni_{39}P_{10}Si_5B_5$, that is ultra-soft magnetic [10]. It is very useful to establish the mechanical as well as the thermal characteristics of the alloy. Furthermore it is very interesting to show the structure development at the early stages of crystallization as it can be crucial for the magnetic characteristics at elevated temperatures and decisive for its potential applications. The present work shows the characterisation of the primary microstructure of the $Fe_{41}Ni_{39}P_{10}Si_5B_5$ arc-melt alloy and focuses on the development of microstructure, thermal stability and mechanical properties of the melt-spun alloy.

2. Experimental

A five component $Fe_{41}Ni_{39}P_{10}Si_5B_5$ alloy was produced using arc melting in argon protective atmosphere from of pure elements: 99.95 wt. % Fe, 99.95 wt. % Ni, 99.999 wt. % Si and Fe-P, Fe-B, Ni-P, Ni-B master alloys. After cutting, grinding and polishing cross-section of the arc-melted droplet of the $Fe_{41}Ni_{39}P_{10}Si_5B_5$ alloy its primary microstructure was observed in (SEM) Philips XL 30 with X-Ray microanalyser Link ISIS-EDX. Then the alloy was melt-spun with a linear rate of 33 m/s. X-Ray diffraction was performed on the DRON-3 diffractometer using CuKα radiation filtered by the LiF bent single crystalization the detector side. The scattering angle 2Θ was varied between 20 and 90 degrees with the constant step of 0.05 degree. Scans were performed in the Θ-2Θ mode. The mechanical properties using CSM Instruments nano-scratch Berkovich tester micro-hardness tester were investigated. The storage modulus E' was investigated by means of differential thermal analysis (DTA: DTA TA Instruments) and dynamic mechanical analysis (DMA: NETZSCH-DMA 242 C). The parameters used for the measurement were as follows: heating rate - 3 K/min, proportional force factor 1.05, maximum dynamic force 2.5 to 7.2 N, constant part of static force 0 N, maximum amplitude ± 20 μm, frequency 1 Hz, sample length 12.1 to 12.7 mm, sample width 2.92 to 3.14 mm, sample thickness 0.026 to 0.030 mm. Differential scanning calorymetry (DSC) measurements were made on DSC 2010 TA Instruments at a heating rate of 20 K/min. Next, the melt-spun alloy was heated up in DSC chamber to 687 K (i.e. the temperature of the first crystallization peak on DSC curve) and investigated by means of the JEOL 300 kV transmission electron microscope (TEM).

3. Results

The results of microstructure SEM/EDS examination of the arc melted droplet are presented on Fig. 1. The primary $Fe_{41}Ni_{39}P_{10}Si_5B_5$ alloy microstructure consists of four constituents i.e.: iron-nickel-silicon dendrities "A" presumably bcc phase, faceted iron-nickel-phosphorus crystals, that are M_3P phosphides "B", nickel-iron-phosphorus regions "C" that located at the tips of iron-nickiel-silicon dendrite arms "A", and the Fe-Ni-Si-base regions "D". The EDS spectrum from "D" regions has a little stronger lines from phosphorus than "A" regions. The "D" regions can possibly be eutectic component as it is located in the intergranular spaces.

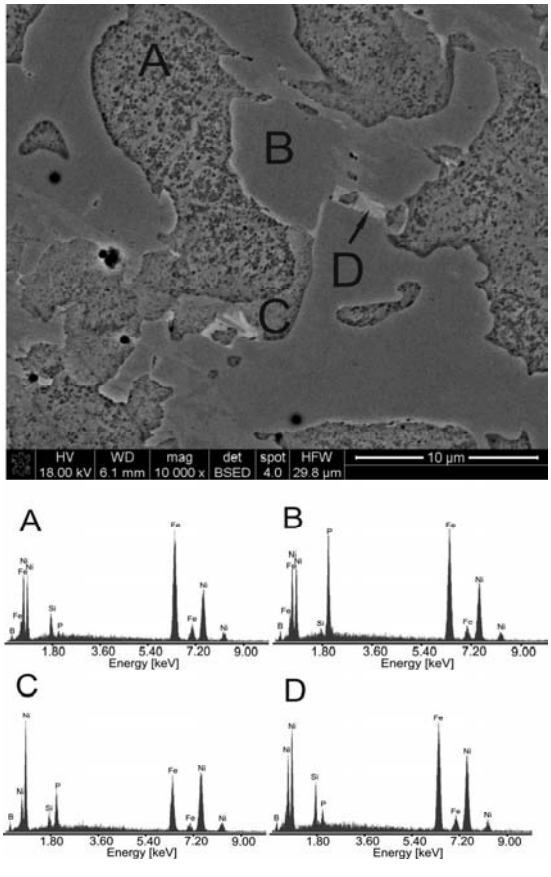

Fig. 1. SEM image for arc-melt $Fe_{41}Ni_{39}P_{10}Si_5B_5$ alloy with EDS analysis for A, B, C and D structural constituents

The results of X-ray diffraction for the $Fe_{41}Ni_{39}P_{10}Si_5B_5$ alloy in melt-spun state represent the two broad diffraction maximums located for 2Θ at between 40° and 50° and between 70° and 90°

(Fig. 2). The diffraction is thus typical for the amorphous state. Therefore, the component multi-phase alloy we produced can be easily vitrified.

The plots of indentation force (F_n) versus displacement (P_d) for a nano-indentation test using 100 mN and the values of Young modulus and Vickers hardness are presented on Fig. 3. The melt-spun alloy presents the hardness number on the level 720 HV and the Young modulus value is 102 GPa. The hardness number is comparable to the values obtained for amorphous $Ni_{80}P_{20}$ (721HV) [11]. However, the Young modulus is higher in the $Fe_{41}Ni_{39}P_{10}Si_5B_5$ alloy than in amorphous $Ni_{80}P_{20}$ (64GPa) [11] i.e. 102GPa therefore the alloying with Fe, Si and B increases the stiffness of the metallic glassy alloy.

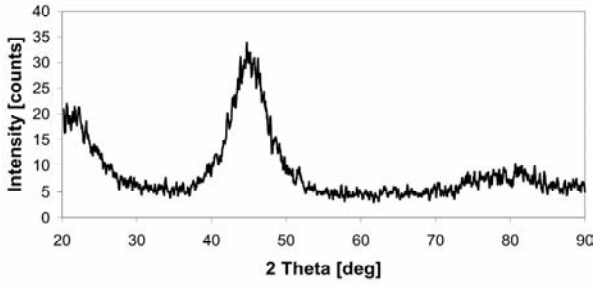

Fig. 2. X-ray diffraction for the $Fe_{41}Ni_{39}P_{10}Si_5B_5$ alloy in melt-spun state

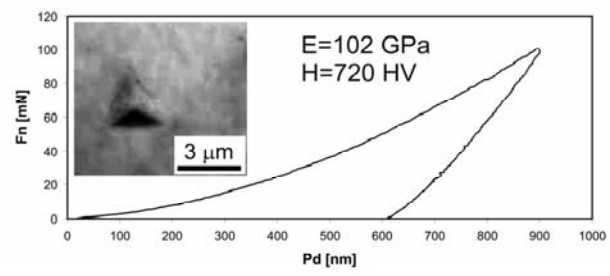

Fig. 3. Indentation curve with Young modulus and hardness results for $Fe_{41}Ni_{39}P_{10}Si_5B_5$ melt spun alloy

The thermal stability and stability of mechanical properties for the $Fe_{41}Ni_{39}P_{10}Si_5B_5$ melt spun alloy are shown on the DSC (Fig. 4) and DMA (Fig. 5) plots. At elevated temperatures up to ca. 550 K there are no significant changes of storage modulus (E') of heat flow. At higher temperatures, there is a substantial drop of storage modulus (E') with the onset at 603 K, and reaches the minimum value of ca. 70 GPa at T_{minE}=654 K. At higher temperatures where DSC plot shows the two exothermic crystallization effects with the onset at T_x=679 K and peak values at 687 K and 743 K, the storage modulus increases to 79 GPa at 747 K. The changes could be well explained and correlated with the gradual decrease of the soft low-viscous glassy matrix and corresponding increase of crystalline products of a higher Young modulus. As the products such as phosphides and borides are very brittle [12, 13], this finally leads to sample breaking above 850 K.

The TEM microstructure of the $Fe_{41}Ni_{39}P_{10}Si_5B_5$ ribbon at the beginning of crystallization process i.e. after heating to the 687 K is presented on Fig. 6. On the basis of the observation it can be assumed that the crystallization of the alloy begins with precipitation of the bcc based crystals that can be iron-based (space group Im-3m). It is possible to distinguish on the diffraction pattern all the strong lines representing the following crystallographic planes: (110), (200), (211), (220), (310).

The course of crystallization is similar to the Fe-Si-B-base [3,14] and Fe-P-Si-B-base [15] amorphous alloys.

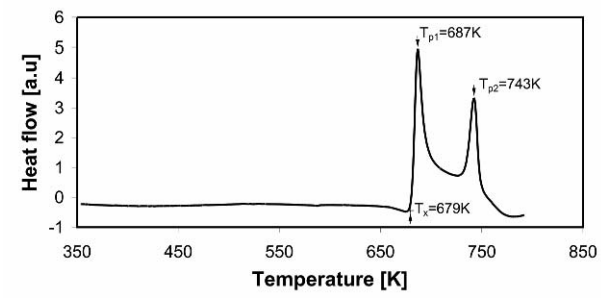

Fig. 4. DSC plot for the $Fe_{41}Ni_{39}P_{10}Si_5B_5$ melt-spun alloy; heating rate 20 K/min

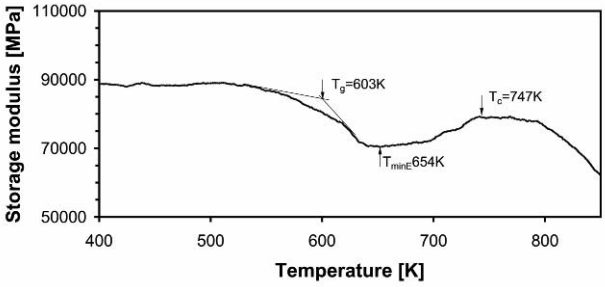

Fig. 5. Storage modulus E' registered at elevated temperatures – DMA curve; heating rate 2.5 K/min

4. Conclusions

- The primary microstructure of the $Fe_{41}Ni_{39}P_{10}Si_5B_5$ alloy consists of four constituents that are: A – Fe-Ni-Si dendrites, B – faceted crystals of M_3P phosphides, C – tips of dendrite arms, D – Fe-Ni-Si-base inter-dendritic regions.
- The $Fe_{41}Ni_{39}P_{10}Si_5B_5$ alloy can be easily vitrified with use of melt-spinning process.
- Hardness value of the $Fe_{41}Ni_{39}P_{10}Si_5B_5$ alloy is on the similar level as in Ni-P based amorphous alloys, however alloying the Ni-P-base composition with with Fe, Si and B gives in the alloy increase of Young modulus in the glassy state.
- The $Fe_{41}Ni_{39}P_{10}Si_5B_5$ melt spun alloy is thermally stable and has the stable mechanical properties up to ca. 550 K. Above that range there is the drop of storage modulus E' caused probably with glass transition. Further heating causes increase of E' due to crystallization.
- The crystallization begins with formation Fe-base bcc nanocrystals and this can be connected with the first exothermic peak on the DSC.

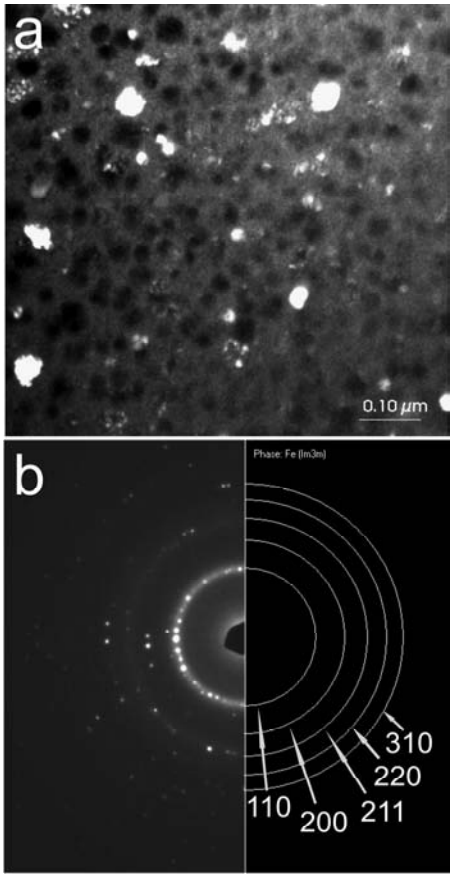

Fig. 6. TEM microstructure (a) with electron diffraction pattern (b) of the $Fe_{41}Ni_{39}P_{10}Si_5B_5$ melt-spun alloy diffraction; the diffraction rings Fe-bcc phase

References

[1] H. Warlimont, Amorphous metals driving materials and process innovations, Materials Science and Engineering A304-306 (2001) 61-61.

[2] A. Inoue, B.L. Shen, C.T. Chang, Super-High Strength of over 4000 MPa for Fe-based Bulk Glassy Alloys in [(Fe1-xCox)0.75B0.2Si0.05]96Nb4 System, Acta Materialia 52 (2004) 4093-4099.

[3] T. Kulik, Nanocrystallization of metallic glasses, Journal of Non-Crystalline Solids 287 (2001) 145-161.

[4] B. Kostrubiec, R. Wiśniewski, J. Rasek, Crystallisation kinetics and magnetic properties of a Co-based amorphous alloy, Journal of Achievements in Materials and Manufacturing Engineering 16 (2006) 30-34.

[5] S. Lesz, D. Szewieczek, J.E. Frąckowiak, Structure and magnetic properties of amorphous and nanocrystalline Fe85.4Hf1.4B13.2 alloy, Journal of Achievements in Materials and Manufacturing Engineering 19 (2006) 29-34.

[6] T. Poloczek, S. Griner, R. Nowosielski, Crystallisation process of Ni-base metallic glasses by electrical resistance measurements, Archives of Materials Science and Engineering 28/7 (2007) 353-356.

[7] S. Lesz, R. Nowosielski, A. Zajdel, B. Kosturbiec, Z. Stokłosa, Investigations of crystallization behaviour of $Co_{80}Si_9B_{11}$ amorphous alloy, Archives of Materials Science and Engineering 28/2 (2007) 91-97.

[8] T.D. Shen, R.B. Swarz, Bulk ferromagnetic glasses in the Fe-Ni-P-B system, Acta Materialia 49 (2001) 837-847.

[9] R. Nowosielski, R. Bobilas, P. Ochin, Z. Stokłosa, Thermal and magnetic properties of selected Fe-based metallic glasses, Archives of Materials Science and Engineering 30/1 (2008) 13-16.

[10] K. Ziewiec, K. Bryła, A. Błachowski, K. Ruebenbauer, K. Prusik, S. Kąc, T. Kozieł, Properties and microstructure of the new Fe-P-Si-base glass forming alloys, Journal of Microscopy, in-press.

[11] K. Ziewiec, J. Dutkiewicz, A. Ziewiec, S. Kąc, The microstructure and mechanical properties of Ni78Ag2P20 alloy, Archives of Materials Science and Engineering 28/11 (2007) 657-660.

[12] K. Ziewiec, J. Lelątko, P. Pączkowski, K. Bryła, Devitrification and Nano-Crystalline/Amorphous Composite Formation in $Ni_{64}Cu_9Fe_8P_{19}$ Glassy Alloy at Elevated Temperatures, Solid State Phoenomena 130 (2007) 167-170.

[13] K. Ziewiec, Properties characterization of the $Cu_{68.5}Ni_{12}P_{19.5}$ alloy at elevated temperatures, Journal of Non-Crystalline Solids 354/33 (2008) 4019-4023.

[14] K. Lu, Nanocrystalline metals crystallized from amorphous solids: nanocrystallization, structure, and properties, Materials Science and Engineering R16 (1996) 161-221.

[15] C.Y. Lin, T.S. Chin, S.X. Zhou, Z.C. Lu, L. Wang, F.F. Chen, M.X. Pan, W.H. Wang, Magnetic properties and glass-forming ability of modified Fe-P-Si-B bulk amorphous alloys, Journal of Magnetism and Magnetic Materials 282 (2004) 156-162.